Thermal Stability of $LiPF_6$ Salt and Li-ion Battery Electrolytes Containing $LiPF_6$

Hui Yang [a,*], Guorong V. Zhuang[b,*,z] and Philip N. Ross, Jr. [b,*]

Environmental Energy Technologies Division[a] and Materials Sciences Division[b]

Lawrence Berkeley National Laboratory

University of California, Berkeley, CA 94720

Abstract

The thermal stability of the neat $LiPF_6$ salt and of 1 molal solutions of $LiPF_6$ in prototypical Li-ion battery solvents was studied with thermogravimetric analysis (TGA) and on-line FTIR. Pure $LiPF_6$ salt is thermally stable up to 380 ^oK in a dry inert atmosphere, and its decomposition path is a simple dissociation producing LiF as solid and PF_5 as gaseous products. In the presence of water (300 ppm) in the carrier gas, its decomposition onset temperature is lowered as a result of direct thermal reaction between $LiPF_6$ and water vapor to form POF_3 and HF. No new products were observed in 1 molal solutions of $LiPF_6$ in EC, DMC and EMC by on-line TGA-FTIR analysis. The storage of the same solutions in sealed containers at 358 ^oK for 300 – 420 hrs. did not produce any significant quantity of new products as well. In particular, no alkylflurophosphates were found in the solutions after storage at elevated temperature. In the absence of either an impurity like alcohol or cathode active material that may (or may not) act as a catalyst, there is no evidence of thermally induced reaction between $LiPF_6$ and the prototypical Li-ion battery solvents EC, PC, DMC or EMC.

---

[*] Electrochemical Society Active Member

[Z] Email: GVZhuang@lbl.gov (GVZ)

Ascend v. Duesenfeld
IPR2024-00948
Ex. 2008-001

Introduction

Lithium hexafluorophosphate ($LiPF_6$) is the most widely used salt in the electrolytes for commercial Li-ion cells. The thermal stability and interaction of this salt with the organic solvents in the electrolytes have been studied experimentally[1-3] by Thermogravimetric Analysis (TGA), Differential Scanning Calorimetry (DSC) and Accelerating Rate Calorimetry (ARC), and computationally by Density Functional Theory (DFT) and Molecular Dynamics (MD) methods[4]. However, all the thermal analysis techniques used so far test thermal stability based on macroscopic quantities such as mass loss, heat flow, or self-heating rate measured as a function of temperature. The results have been inconsistent in part because the temperatures at which thermally activated processes were observed differed significantly depending on the thermal analysis method used. For example, as measured by DSC[2,3] the temperature for onset of thermal decomposition of the neat salt $LiPF_6$ was 573 ^{o}K in a heretically sealed sample pan and 450 ^{o}K at ambient pressure. In related ambient pressure experiments[1,2], the onset temperature varied by as much as 130 ^{o}K between DSC and TGA measurements. In addition, the identification of the decomposition products is also the subject of debate in the literature[5,6]. While both Armand and Abraham agreed that thermal dissociation of EC:$LiPF_6$ solvent alone does not produce fluoro-organics, they disagreed on the nature of catalysts which activate the formation of fluoro-organics during storage at elevated temperature ~ 85 ^{o}C. Armand attributed a catalytic effect to cathode active material (e.g. $LiCoO_2$ and $LiNiO_2$), while Abraham et al. attributed production of fluoro-organics in DEC:$LiPF_6$ electrolyte to a catalytic effect of POF_3 generated by reaction of alcohol

Duesenfeld Ex. 2008-002

impurities with PF_5. Clearly, the thermochemistry of the commonly used Li-ion battery electrolytes still needs further elucidation.

In this study, we use TGA and on-line FTIR to investigate the thermal stability of neat $LiPF_6$ in both an inert gas environment and with water added to the inert gas (300 ppm), as well as thermal reaction of the salt and a variety of alkyl carbonate solvents (EC, PC, DMC and EMC) up to 570 ^oK in the absence of any purported catalytic agents.

Experimental

$LiPF_6$ (Aldrich, 99%) and 1 m (molal) $LiPF_6$ /ethylene carbonate (EC), 1 m $LiPF_6$ /ethyl methyl carbonate (EMC) and 1 m $LiPF_6$ /dimethyl carbonate (DMC) were used as received. The solutions were supplied by the Army Research Lab (Adelphi, MD). The water content of all the electrolytes is less than 10 ppm. All the sample handlings were performed in inert atmosphere with no air exposure even momentarily.

The TGA-FTIR was a Thermo-Gravimetric Analyzer (Model 2960, TA Instruments) with on-line gas analysis by a Fourier Transform Infrared (FTIR) Spectrometer (Nexus 470, Nicolet) equipped with a temperature-controlled transmission gas cell. The coupling between TGA and FTIR is via heated quartz capillary. Both FTIR gas cell and capillary were heated to 473 ^oK during experiments to prevent deposits on their walls. To ensure a dry inert atmosphere environment, the entire TGA and FTIR gas cell were housed in argon-purged glovebag. Special care was taken to ensure that the FTIR optical path was properly purged such that the background signal from residual moisture and carbonate dioxide (CO_2) is negligible during the experiments. The inert working condition of the entire apparatus was checked using thermal decomposition of a copper oxalate sample, as recommended by Mullen et al.[7].

The TGA-FTIR setup measures the change in sample weight as a function of temperature while simultaneously monitoring the volatile components evolved from samples as a result of thermal decomposition. The measurement can be performed under either isothermal or non-isothermal conditions. Under the non-isothermal condition, the sample is heated at a controlled rate, typically 10 ^{o}K /min., until the mass loss is negligible. The isothermal experiments were carried out by ramping the sample temperatures to a target temperature, followed by holding the temperature for one hour. The target temperature was then increased sequentially until the sample has decomposed completely. The gas phase products were continuously swept (flow rate of 220 ml/min) into the FTIR gas cell using either high purity argon (Research Grade, less than 10 ppm water) as carrier gas, or argon with water vapor added to 300 ppm. The FTIR spectra were continuously acquired at a resolution of 4 cm^{-1} and summed over 32 scans during the thermogravimetric (TG) measurements. The mass loss reported in this work has ±1% accuracy.

For long-term stability experiments, 1m $LiPF_6$/EC, 1m $LiPF_6$/DMC and 1m $LiPF_6$/EMC electrolytes were stored under vacuum (< 30 mTorr) in high density polypropylene bottles, and heated to 358 ^{o}K for 420 hours for cyclic carbonates and 300 hours for linear carbonates. The compositions of the electrolytes were then measured by FTIR using the Attenuated Total Reflection (ATR) method[8]. The spectra were acquired at resolution of 4 cm^{-1} and total scans of 512.

Results and Discussion

Thermal Decomposition pathway of $LiPF_6$

Thermogravimetry (TG) profiles of pure $LiPF_6$ salt obtained, at a heating rate of 10 ^oK /min., with carrier gas containing less than 10 ppm of water (solid line) and with 300 ppm of water (dashed line), respectively, follow similar trends as shown in Fig. 1 (A). The effect of water on the TG profile deviation is subtle, with a comparable (ca. 17%) mass remaining when temperature reaches 530 ^oK. However, the influence of water vapor is demonstrated more clearly by the derivative thermogravimetry (DTG) profile, i.e. dm/dT verses T plot, which indicates a clearly defined shift in the TG inflection point when 300 ppm of water is present in the carrier gas. Also apparent in the DTG is a decreasing of the onset temperature for mass loss (inset of Fig.1 (A)) by ca. 27 ^oK in the presence of 300 ppm water vapor. As shown in the differential thermal analysis (DTA) trace (Fig.1 (B)), thermal decomposition of $LiPF_6$ is an endothermic process. A small endothermic peak at ca. 470 ^oK superposed on the main peak can be attributed to the melting of $LiPF_6$ based on observation of an endothermic peak at the same temperature by Differential Scanning Calometry (DSC). The decomposition enthalpy and melting enthalpy are reported to be ca. 84.27 kJ/mol [2] and 2.61±0.03 kJ/mol [9], respectively.

The presence of water vapor did have a significant effect on the composition of gaseous products during decomposition/volatilization. The typical FTIR spectrum of initial decomposition products of $LiPF_6$ at 488 K in dry conditions (< 10 ppm water) is shown in Fig. 2 (A). Spectral features of strong intensity are observed at 1018 cm^{-1} and 945 cm^{-1}, along with weak features at 574 cm^{-1} and 534 cm^{-1}. The comparison between experimental measured and calculated vibrational frequencies of PF_5 suggests that all of the features in this spectrum could be attributed to vibrational modes of PF_5, as summarized in Table Ia. With the carrier gas containing 300 ppm water vapor, other

products are observed in addition to PF_5, as shown in Fig. 2 (B) at 479 ^oK. A series of rotational bands spanning 4300 – 3600 cm^{-1} are characteristic of vapor phase hydrofluoric acid (HF), consistent with stretching frequency predicted from force constant of F-H[10]. In addition, strong absorption peaks are observed at 1416 cm^{-1}, 989 cm^{-1} and 473 cm^{-1}, along with weak features at 872 cm^{-1} and 483 cm^{-1}. The peak at 821 cm^{-1} (marked by asterisk) originated from a solid residue on the IR cell wall and not from gas phase product in this case. By comparing these spectral features with vibration frequencies of phosphorous oxyfluoride (POF_3) from our molecular orbital (MO) calculations (see Table Ib), we could readily assign the peak at 1416 cm^{-1} to a P=O stretching mode, and those at 989 cm^{-1} and 871 cm^{-1} to asymmetric and symmetric stretching mode of the $=PF_3$ group, respectively. The peak at 483 cm^{-1} is attributed to a $=PF_3$ bending mode, while coupling of P=O and $=PF_3$ bending modes gives rise to the peak at 473 cm^{-1}.

The relative concentrations of gases extracted from the IR spectra acquired during the TG analysis could be easily related to sample weight loss. The selected infrared peak intensities (PF_5 1018 cm^{-1}; POF_3 1416 cm^{-1}; HF 4038 cm^{-1}) representative of each gas phase products during $LiPF_6$ thermal decomposition are shown in Fig. 3. Clearly, in the dry carrier gas, PF_5 (solid line) is the only gas phase product detected by FTIR in the entire temperature range of 380 ^oK –540 ^oK. The weight percent of the remaining solid product at the end of TG analysis was 17.1% of initial mass, in good agreement with calculated lithium fluoride (LiF) to $LiPF_6$ mass ratio in the reaction

$$LiPF_6 \rightarrow LiF + PF_5 \qquad [1]$$

Duesenfeld Ex. 2008-006

Therefore, the $LiPF_6$ thermal decomposition path is the simple dissociation of the salt under dry (< 10 ppm) conditions. In contrast, in the presence of 300 ppm water vapor in carrier gas, besides PF_5, a significant amount of POF_3 and HF are produced across a wide temperature range, and their evolution profile follows similar trend as a function of temperature (dashed lines in Fig. 3), indicating that they are produced simultaneously. The evolution of HF and POF_3 prior to PF_5 could only be the result of direct reaction between $LiPF_6$ and moisture, i.e.,

$$LiPF_6 + H_2O \rightarrow LiF + POF_3 + 2HF \qquad [2]$$

The insert in Fig. 3 shows that the onset temperature for this reaction is ca. 27 °K lower than that of dissociation to PF_5 (~ 390 ^{o}K) in dry conditions. Interestingly, there is also a delay/shift to higher temperature and an overall reduction of normalized IR peak intensity of PF_5 in the presence of water. This may due to PF_5 reaction with water in the carrier gas via.

$$PF_5 + H_2O \rightarrow POF_3 + 2HF \qquad [3]$$

At temperatures above 390 ^{o}K, the evolution of HF and POF_3 persists, most likely proceeding simultaneously via reactions [2] and [3] until all the $LiPF_6$ is completely converted into LiF.

The TG analysis of $LiPF_6$ at isothermal conditions was carried out to determine the possibility of kinetically slow processes that may be difficult to observe in non-isothermal measurements. As shown in Fig.4, in the dry gas there is apparently no mass change within one hour at 343 ^{o}K or 363 ^{o}K, and only 3.2% mass loss is observed after one additional hour at 383 ^{o}K. These results clearly demonstrated that $LiPF_6$ is thermally stable up to 363 ^{o}K in a dry environment. The onset temperature under isothermal

condition of ca. 383 ^{o}K is in excellent agreement with that obtained from the non-isothermal experiment.

Thermal Gravimetric Analysis of solutions of $LiPF_6$ salt in EC and PC

The TGA-FTIR analysis of the $LiPF_6$/EC solution with dry carrier gas (< 10 ppm water) is shown in Fig. 5 (A), where virtually all the spectral features originate from vapor phase EC and PF_5. The shape of the PF_5 evolution peak is nearly identical to that for the neat salt. The mass remaining at 570 K was 3%, in good agreement with the mass ratio of LiF in $LiPF_6$/EC (3.6%), and well within the 1 % accuracy of the instrument. Therefore, there is no indication of any reaction between EC and $LiPF_6$. The continued evolution of EC after PF_5 formation is complete presumably comes from EC:LiF solvate. With water vapor in the carrier gas, the profiles in Fig. 5 (B) in comparison to those in Fig. 3 reveal that the evolution of POF_3 and HF from the $LiPF_6$/EC solution were changed very little by the presence of EC, indicating the water reacts with $LiPF_6$ via reaction path [2] and reaction path [3] essentially unimpeded by the EC. The result also implies that the POF_3 and HF gases do not react further with the EC to form other products, at least under these non-isothermal (dynamic) conditions. TGA-FTIR analysis of $LiPF_6$/PC produced results essentially identical to those shown for $LiPF_6$/EC system. During TG analysis up to 570 °K, we found no evidence of gaseous products formed by reactions between the cyclic carbonates EC and PC and $LiPF_6$, or its decomposition products, such as PF_5, POF_3 and HF. In particular, there was no evidence of carbon dioxide (CO_2), for which the IR analysis is particularly sensitive. However, reactions that do not result in weight loss and gaseous products would not be detected by the TGA-FTIR experiment, e.g. thermal reaction via acid-catalyzed ring-opening polymerization of

EC could not be easily detected. Nonetheless, if the polymerization of EC did proceed, there would be simultaneous CO_2 evolution. Even with very high IR sensitivity for CO_2, we did not detect any trace of CO_2 release during the TGA experiment, and the mass of the solid residue was consistent with LiF as the only solid product formed.

Thermal stability of solutions of $LiPF_6$ salt in DMC and EMC

TGA-FTIR analysis of 1m $LiPF_6$/EMC and 1m $LiPF_6$/DMC solutions did not yield meaningful results. The evaporation of the solvents in these solutions into flowing carrier gas is so rapid at low temperature (< 400 ^oK) that there is little or no solvent left to react with the salt as it dissociates. More meaningful results for these solutions were obtained from FTIR analysis of the solutions after storage at elevated temperature. The spectral comparison of 1m $LiPF_6$/EC before (spectrum a) and after storage (spectrum b) is presented in Fig. 6. No new features or changes induced by elevated temperature are observed within the detection limit of FTIR. Even after deliberately adding 300 ppm of H_2O, the electrolyte spectrum (c in Fig. 6) is nearly unchanged from that of the starting solution. There is a new small peak in the C-H region at 2850 cm^{-1}, which could be assigned to aliphatic methylene group ($-CH_2-$) symmetric stretching mode (the asymmetric stretching mode would fall under the strong EC peak at 2933 cm^{-1}) and would be indicative of ring-opening cleavage of EC. However, by scaling the peak intensity (0.0008 abs. units) of aliphatic ($-CH_2-$) with that of ($-CH_2-$) EC at 2933 cm^{-1} (0.0175 abs. units), the upper limit of EC cleavage was estimated to be 5% of the total EC for the electrolyte with 300 ppm of water added.

IR spectra of solutions of $LiPF_6$ in the single component linear carbonate solvents DMC and EMC after storage at 358 ^oK for 300 hours are shown in Figures 7 and 8,

respectively. The interpretation of these spectra is complicated by a stronger effect of ion solvation on characteristic vibrations of both the PF6 anion and the solvent molecules than in EC. A discussion of the reasons for these differences is beyond the scope of this work, and will be the subject of a separate paper. The shifts due to ion solvation are seen in the comparison of the a-b spectra: new band on the low frequency side of the carbonyl group (C=O) vibration at 1750 cm^{-1}; new band on the high frequency side of the carbonate group O-C-O asymmetric stretching mode at 1266 cm^{-1}; a new band on the high frequency side of the C-H stretch of the methoxy group at 2860 cm^{-1}; and a splitting of the P-F stretching band of $(PF_6)^-$ anion in EC (at 843 cm^{-1}) into two bands in DMC and EMC that we attribute to ion-pairing in the latter solvents. However, the subsequent spectra (c and d) after high temperature storage either with (d) or without (c) added water show no new bands. The increases in relative intensity of the ion solvation side bands are due to evaporation of solvent from the containers that were not (as it turns out) hermetically sealed. What is **not** observed is a characteristic band of alkylflurophosphates, e.g. OPF_2OR and/or $OPF(OR)_2$ where R could be either methyl or ethyl. The presence of alkylflurophosphates would give rise to three characteristic absorption bands in spectral region of 1320-1140 cm^{-1}, 1088-920 cm^{-1} and 890-805 cm^{-1}, respectively. The 1320-1140 cm^{-1} band is from P=O stretching mode and its exact position varies with the sum of the Pauling electronegativities of the attached groups[11]. The 1088-920 cm^{-1} band, with intensity comparable or stronger than that of the1320-1140 cm^{-1} band, originates from P-O-C (aliphatic carbon) mode[12-13]. The P-F stretching mode in organic phosphorous-fluorine compounds is in the same frequency region as the PF_6 anion [10]. Although it appears that there are some subtle changes in the P-F region

after elevated temperature storage, the absence of a new strong peak between 1088-920 cm^{-1} region definitely exclude the alkylflurophosphates or compounds containing aliphatic P-O-R (R= alkyl group) moieties. Therefore, we conclude that in the absence of either an impurity like alcohol or cathode active material that may (or may not) act as a catalyst there is no evidence of thermally induced reaction between $LiPF_6$ and prototypical Li-ion battery solvents EC, DMC or EMC even in the presence of water.

Summary

Pure $LiPF_6$ salt is thermally stable up to 380 K in a dry (< 10 ppm water) inert atmosphere, and its decomposition path is a simple dissociation producing LiF as solid and PF_5 as gaseous products. In the presence of water (300 ppm) in the carrier gas, its decomposition onset temperature is lowered to about 360 ^oK as a result of direct thermal reaction between $LiPF_6$ and water vapor to form POF_3 and HF. 1 molal solutions of $LiPF_6$ in EC, DMC and EMC were heated in inert carrier gas to 540 ^oK (10 ^oK/ sec) and no new products were observed by on-line FTIR analysis that would indicate reaction between the salt and solvent. This was the case even in the presence of 300 ppm water in the carrier gas. In particular, no CO_2, for which the FTIR analysis is extremely sensitive, was detected. The storage of the same solutions in sealed containers at 358 ^oK for 300 – 420 hrs. did not produce any significant quantity of new products that would indicate reaction between the salt and solvent. However, there was some evidence of EC ring-cleavage in the solution containing 300 ppm water, but less than 5 % of the EC would have been involved. In particular, no alkylflurophosphates were found in the DMC or EMC solutions after storage at elevated temperature even in the presence of water.

Therefore, we conclude that in the absence of either an impurity like alcohol or cathode active material that may (or may not) act as a catalyst there is no evidence of thermally induced reaction between $LiPF_6$ and prototypical Li-ion battery solvents EC, DMC or EMC.

Acknowledgement

This work was supported by the Assistant Secretary for Energy Efficiency and Renewable Energy, Office of FreedomCAR and Vehicle Technologies of the U.S. Department of Energy under contract No. DE-AC02-05CH11231. We thank Drs. K. Xu, S. S. Zhang and T. Richard Jow of the Army Research Lab for supplying electrolytes used in this work.

Duesenfeld Ex. 2008-012

References

1. S. E. Sloop, J. K. Pugh, S. Wang, J. B. Kerr, and K. Kinoshita, *Electrochem. Solid-State Lett.,* **4**, A42 (2001).

2. K. S. Gavritchev, G. A. Sharpataya, A. A. Smagin, E. N. Malyi and V. A. Matyukha, *J. Therm. Anal. Cal.*, **73**, 71 (2003).

3. D. D. MacNeil and J. R. Dahn, *J. Electrochem. Soc.*, **150**, A21 (2003).

4. K. Tasaki, K. Kanda, S. Nakamura and M. Ue, *J. Electrochem. Soc.*, **150**, A1628 (2003).

5. A. Hammami, N. Raymond and M. Armand, *Nature*, **424,** 635 (2003).

6. C. L. Campion, W. Li, W. B. Euler, B. L. Lucht, B. Ravdel, J. F. DiCarlo, R. Gitzendanner and K. M. Abraham, *Electrochem. Solid-State Lett.,* **7**, A194 (2004).

7. J. Mullens, A. Vos, R. Carleer, J. Yperman, L. C. Can Poucke, *Thermochim. Acta,* **207**, 337 (1992).

8. G. V. Zhuang, P. N. Ross, Jr., *Electrochem. Solid-State Lett*., **6**, A136 (2003).

9. Hui Yang, Ph. D. Thesis, Illinois Institute of Technology, 2003.

10. N. B. Colthup, L.H. Daly and S.E. Wiberley, *Introduction to Infrared and Raman Spectroscopy*, 3rd Ed., Academic Press (1990).

11. J. V. Bell, J. Heisler, H. Tannenbaum and J. Goldenson, *J. Am. Chem. Soc.*, **76**, 5185 (1954).

12. L. C. Thomas [1] and R. A. Chittenden, *Spectrochim. Acta*, **20,** 467 (1964).

13. L. C. Thomas [2] and R. A. Chittenden, *Spectrochim. Acta*, **20,** 480 (1964).

Table I. POF_3 and PF_5 Experimental Vibrational Frequencies Assignments

Table Ia. Vibrational Frequencies of PF_5		
Calculated (cm^{-1})	Experimental (cm^{-1})	Assignment
946	1018	PF(1) stretching mode
904	945	PF(2) stretching mode
512	574	PF(1) bending mode
475	534	PF(2) bending mode

Table Ib. Vibrational Frequencies of POF_3		
Calculated (cm^{-1})	Experimental (cm^{-1})	Assignment
1329	1416	P=O stretching mode
909	989	PF asymmetric stretching mode
789	871	PF symmetric stretching mode
431	483	PF_3 bending mode
421	473	PF_3 & P=O bending mode

Figure captions

Figure 1. (A) mass loss (left) and rate of mass loss (right) during thermal decomposition of $LiPF_6$ at a heating rate of 10 °K/min. in argon (flow rate: 220 ml/min) containing < 10 ppm H_2O (solid line) and with 300 ppm water vapor (dashed line); (B) derivative thermal analysis (DTA) profile in the same experiment.

Figure 2. FTIR spectra of gaseous products from $LiPF_6$ decomposition at T = 488 °K in low moisture environment (A) and at T = 479 °K in environment containing 300 ppm water vapor (B). Spectrum in (A) is assigned entirely to PF_5 and (B) to a mixture of POF_3 and HF (see Table 1 for details).

Figure 3. Evolution of gaseous products as a function of temperature during thermal decomposition of $LiPF_6$ at a heating rate of 10 °K /min in argon (flow rate: 220 ml/min.) containing less than 10 ppm water (solid line) and with 300 ppm water vapor (dashed line).

Figure 4. Isothermal curves of $LiPF_6$ decomposition from 343 °K to 423 °K at temperature intervals of 20 °K in dry (<10 ppm H_2O) carrier gas.

Figure 5. Gaseous products distribution of 1 m $LiPF_6$/EC solution obtained from on-line TGA-FTIR at a heating rate of 10 °K /min in argon (flow rate: 220 ml/min.): (A) dry (< 10 ppm water) and (B) with 300 ppm water vapor in the argon.

Duesenfeld Ex. 2008-015

Figure 6. FTIR spectra in (A) 2000-700 cm^{-1} and (B) 3150-2750 cm^{-1} regions of: (a.) 1m $LiPF_6$ /EC solution; (b.) after storage at 358 °K for 420 hours in a closed container; (c.) same storage experiment with 300 ppm H_2O added.

Figure 7. Same experiment as in Figure 6 for 1 m $LiPF_6$/DMC: (a.) pure DMC; (b.) 1 m $LiPF_6$/DMC solution; (c.) after storage at 358 °K for 300 hours; (d.) with 300 ppm H_2O added.

Figure 8. Same experiment as in Figure 6 for 1m $LiPF_6$/EMC solution: (a.) pure EMC; (b.) 1m $LiPF_6$/EMC solution; (c.) after storage in closed container under vacuum at 358 °K for 300 hours (d.) with 300 ppm H_2O added.

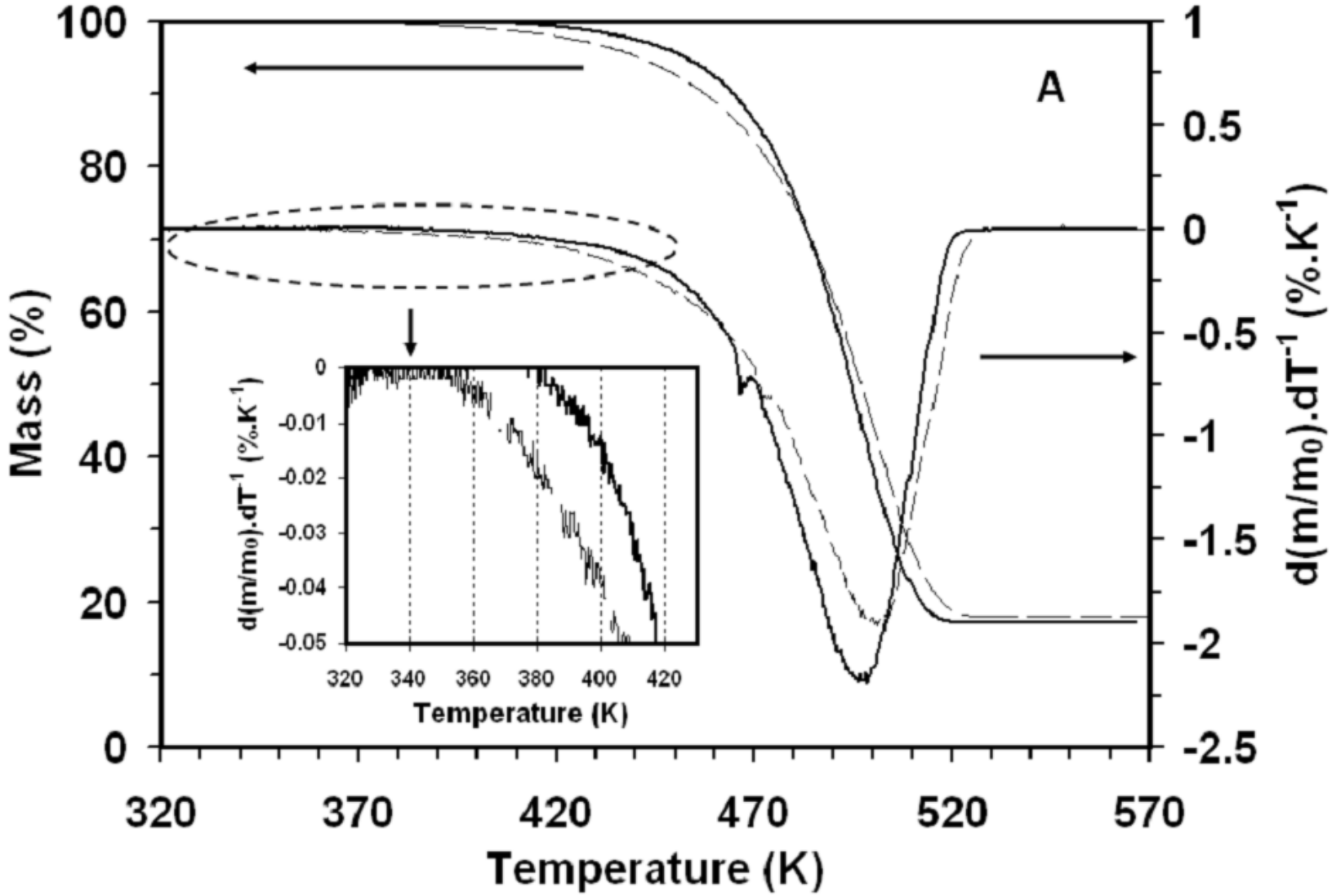

Duesenfeld Ex. 2008-017

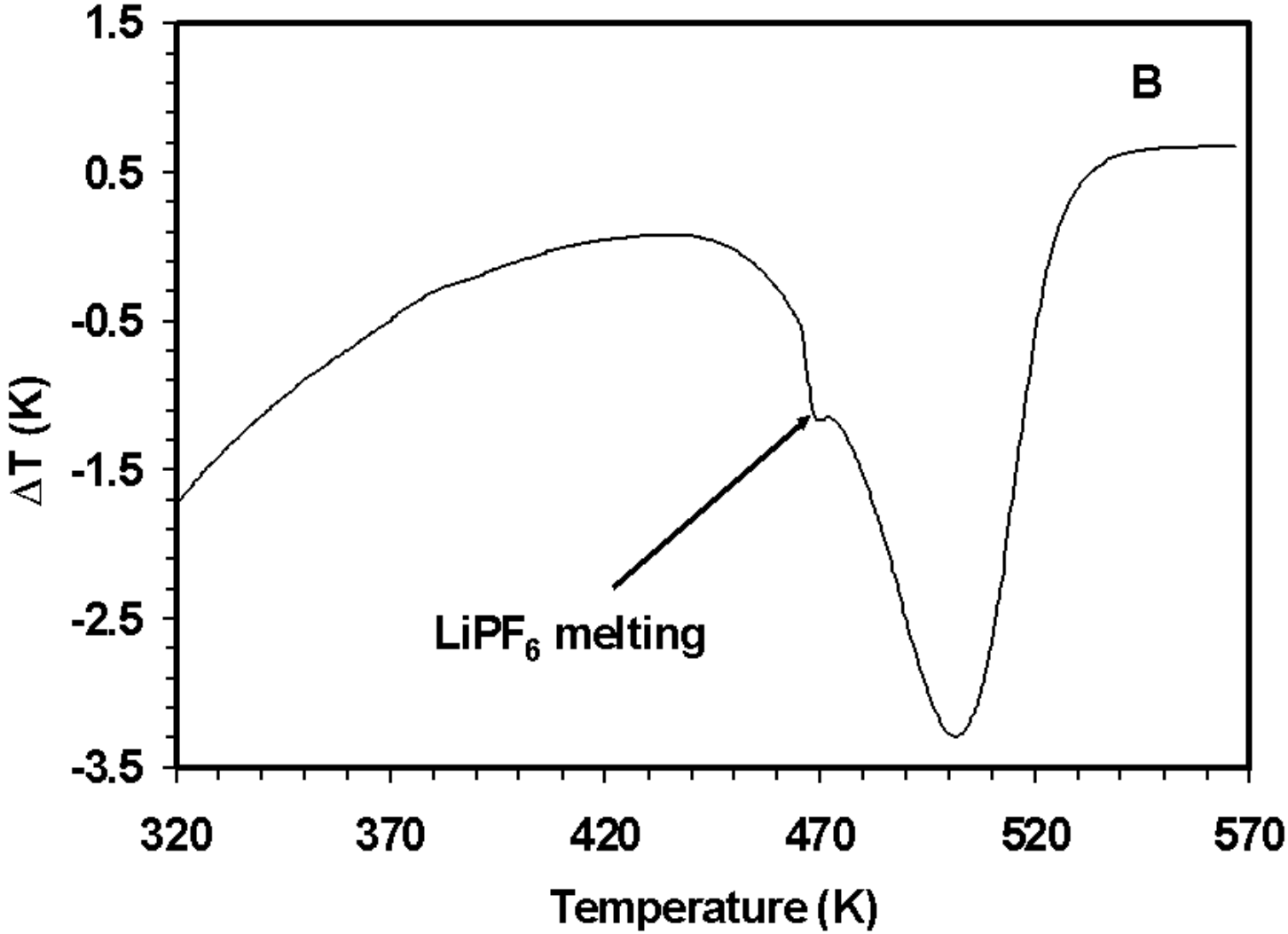

Duesenfeld Ex. 2008-018

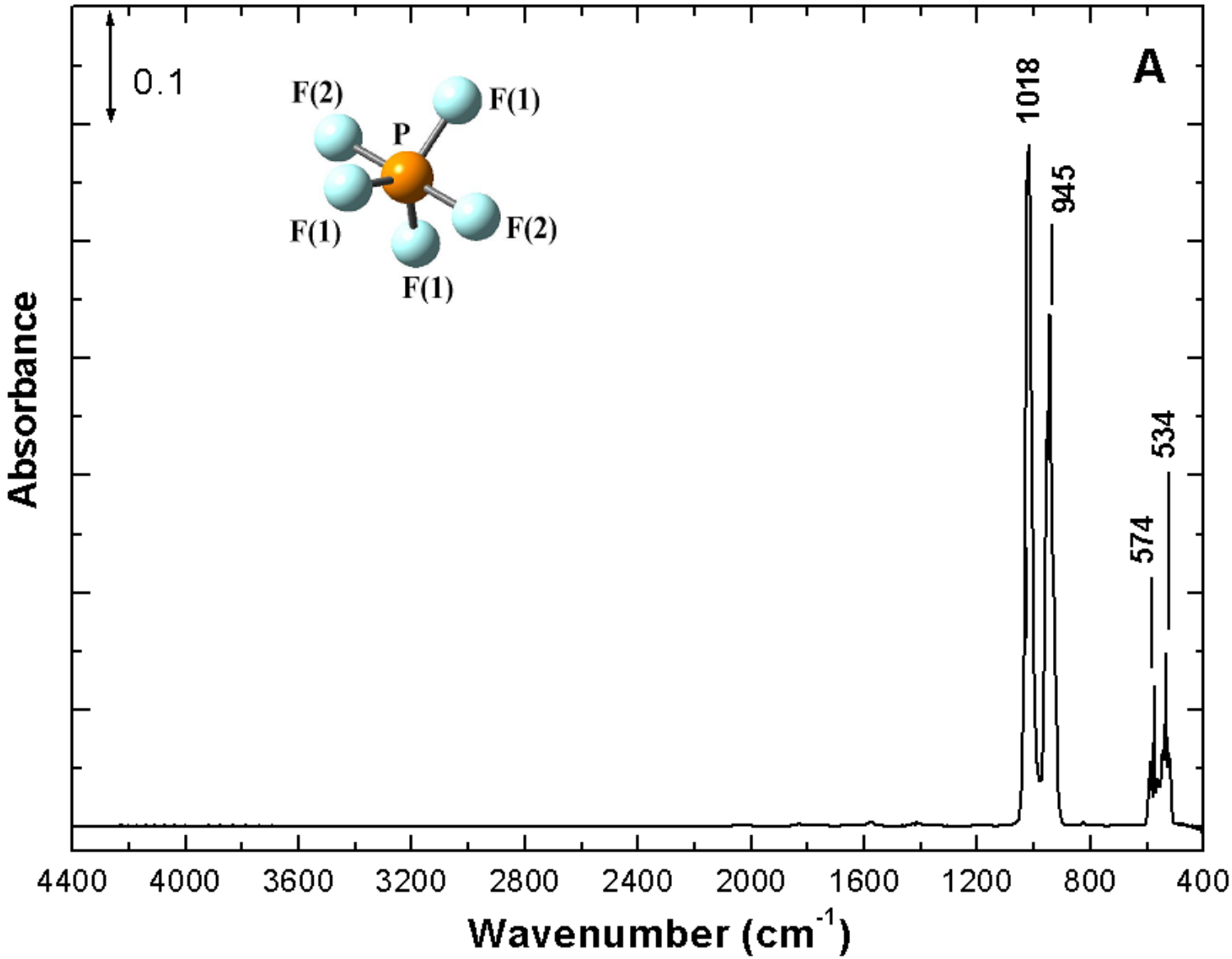

Duesenfeld Ex. 2008-019

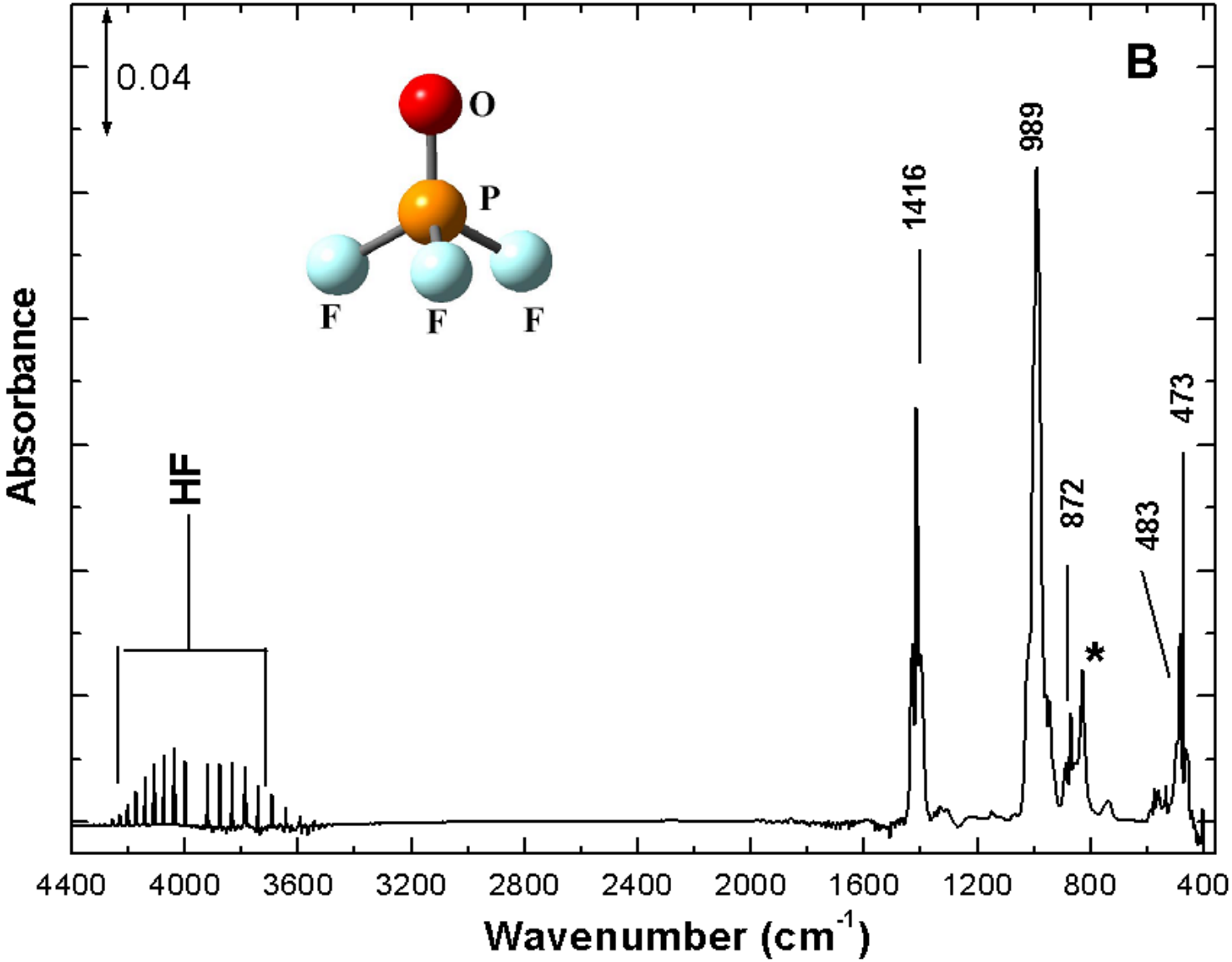

Duesenfeld Ex. 2008-020

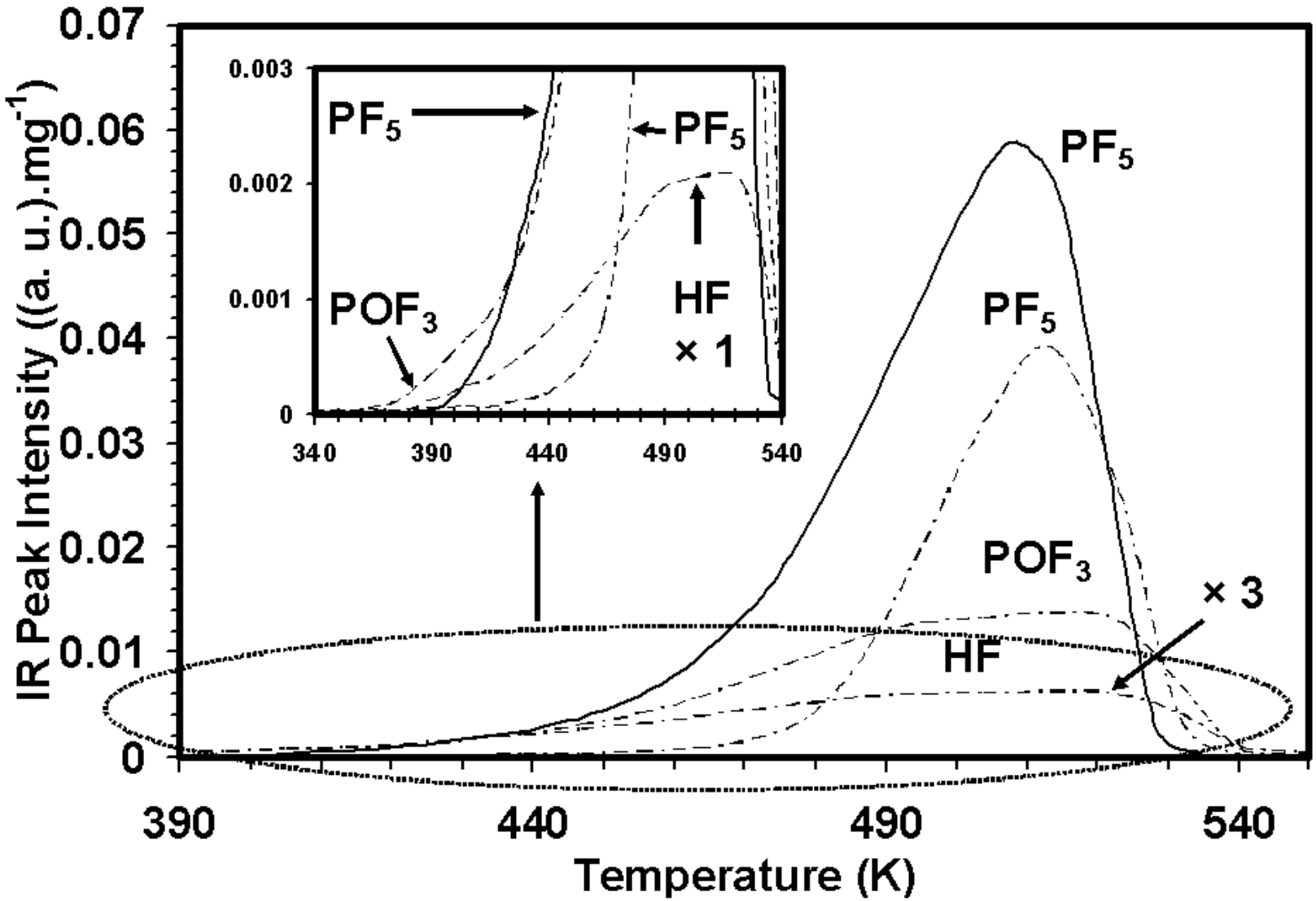

Duesenfeld Ex. 2008-021

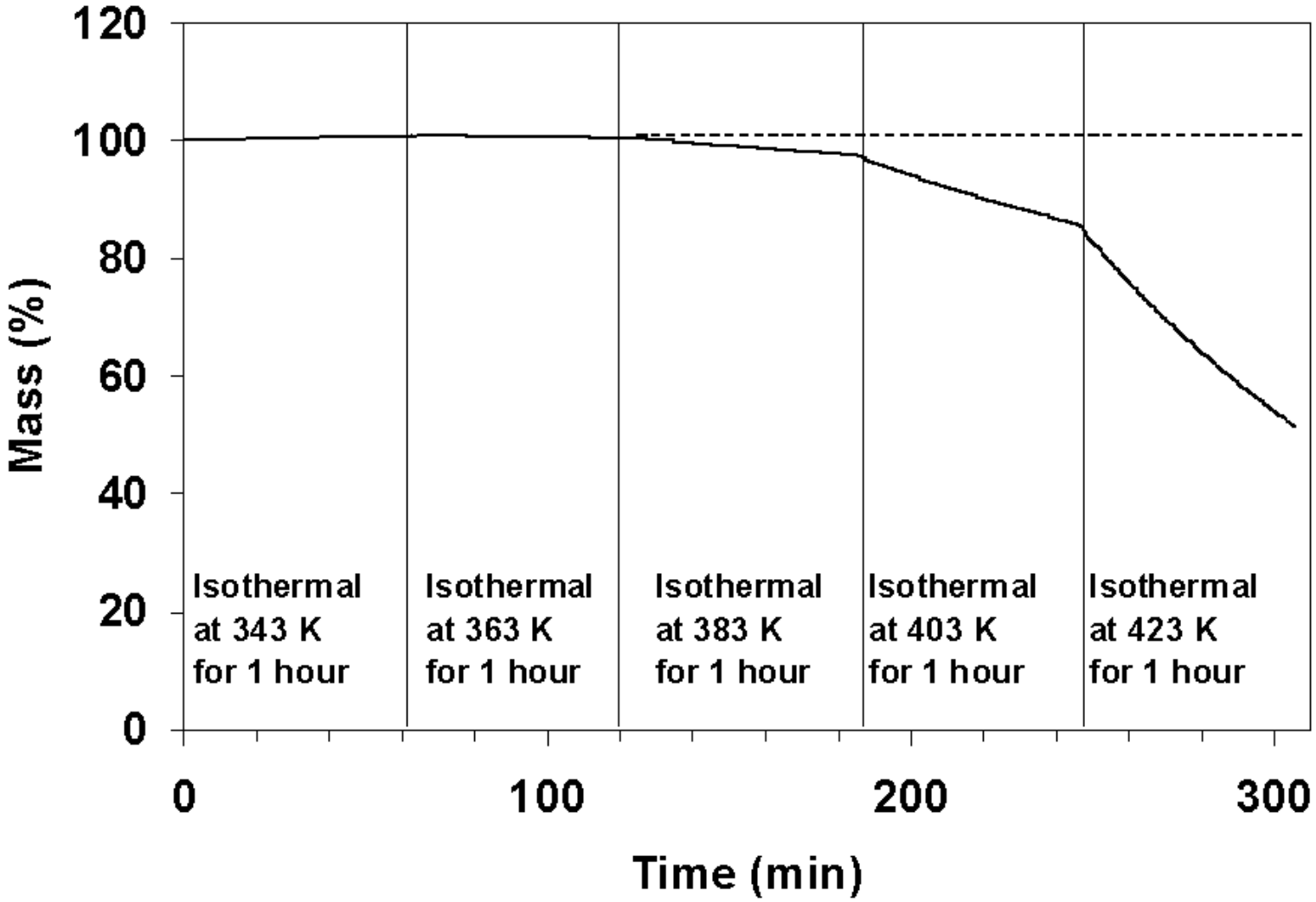

Duesenfeld Ex. 2008-022

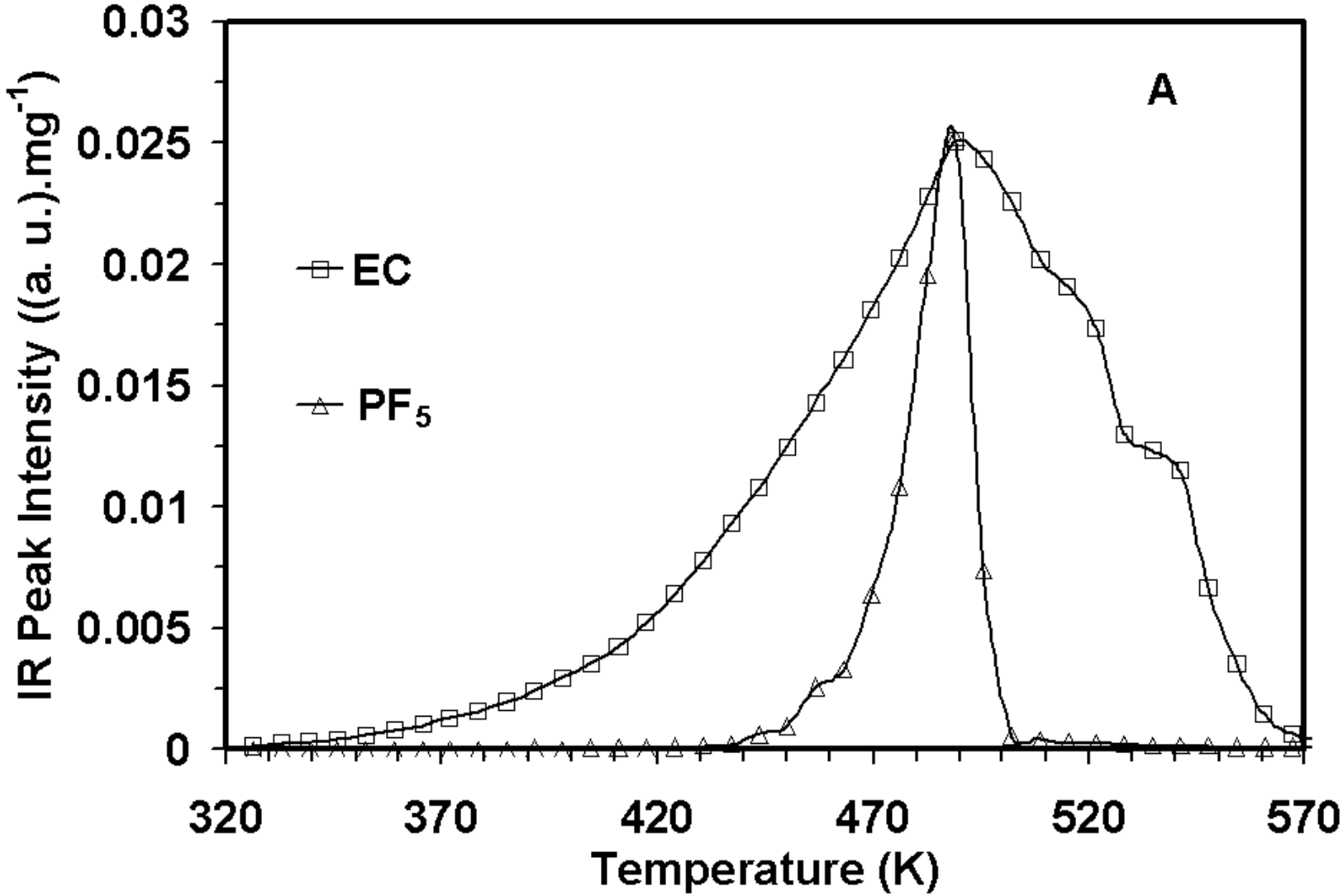

Duesenfeld Ex. 2008-023

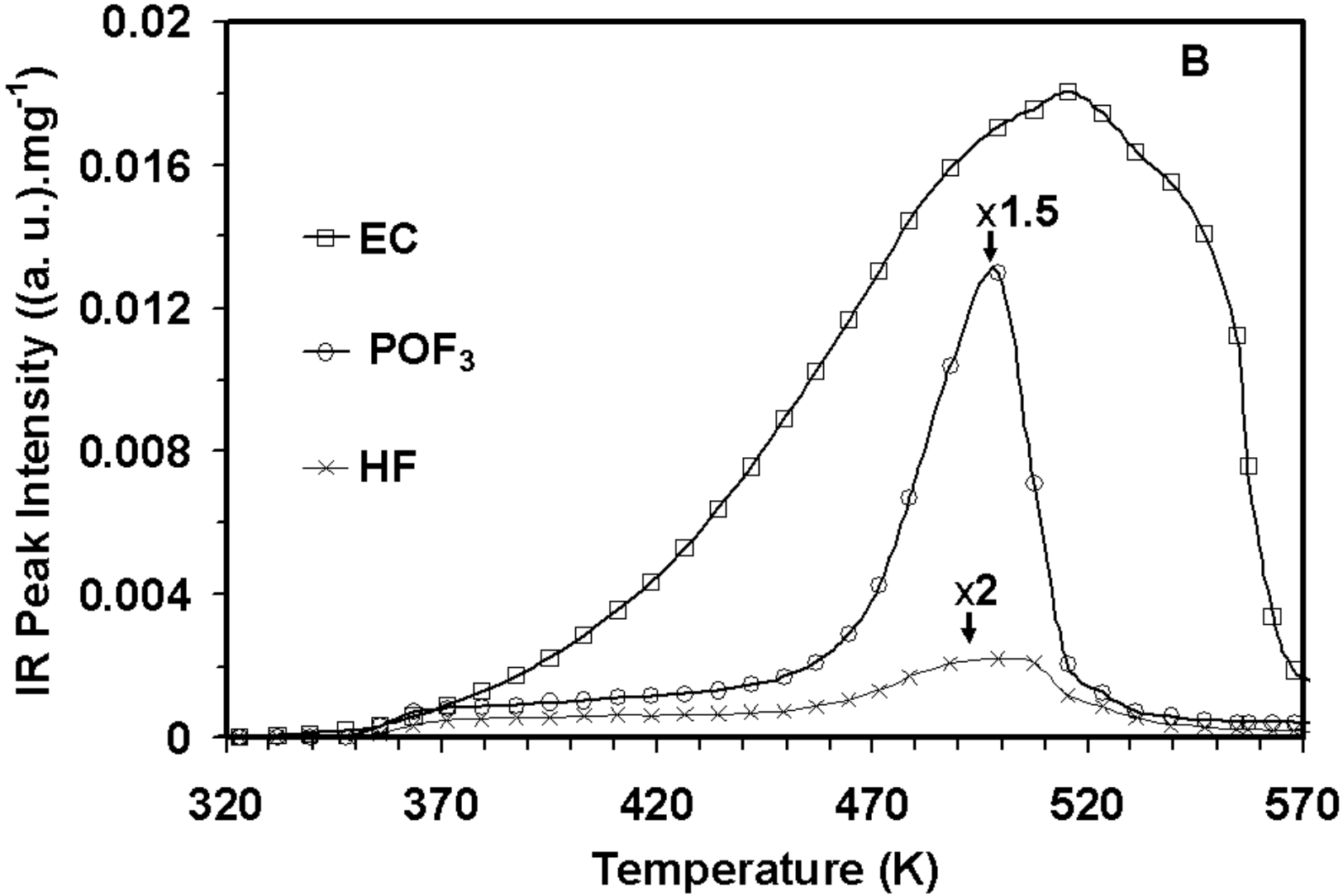

Duesenfeld Ex. 2008-024

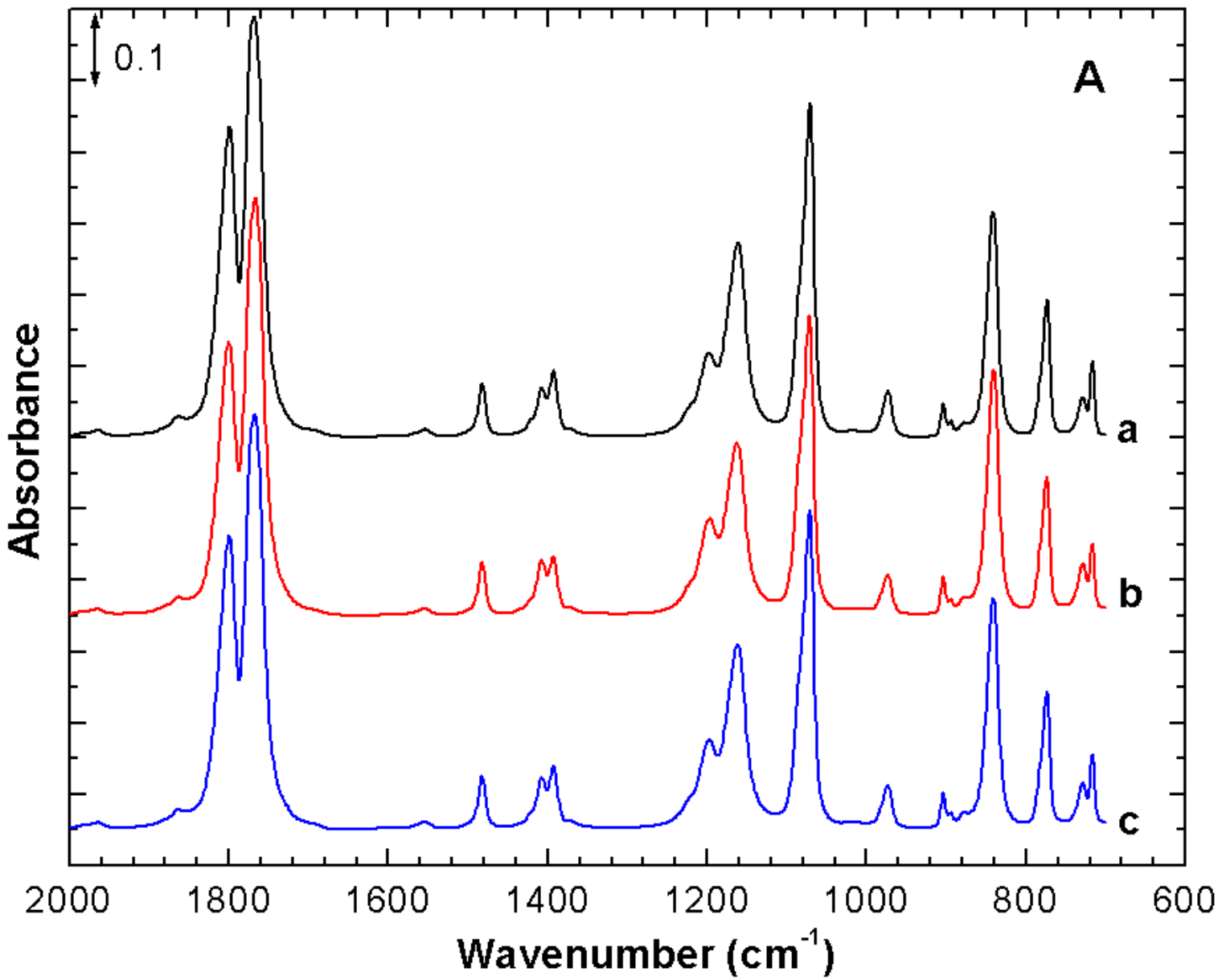

Duesenfeld Ex. 2008-025

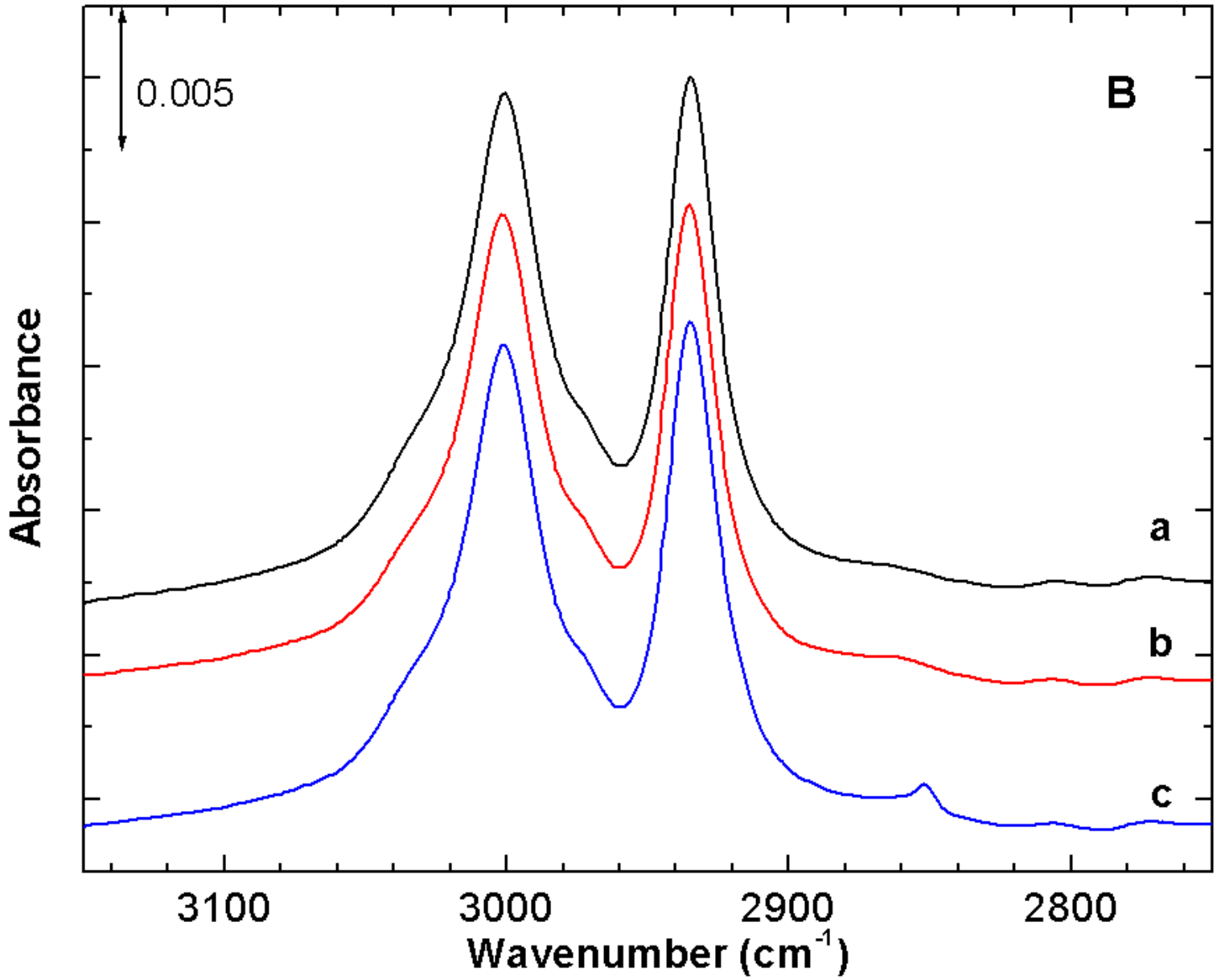

Duesenfeld Ex. 2008-026

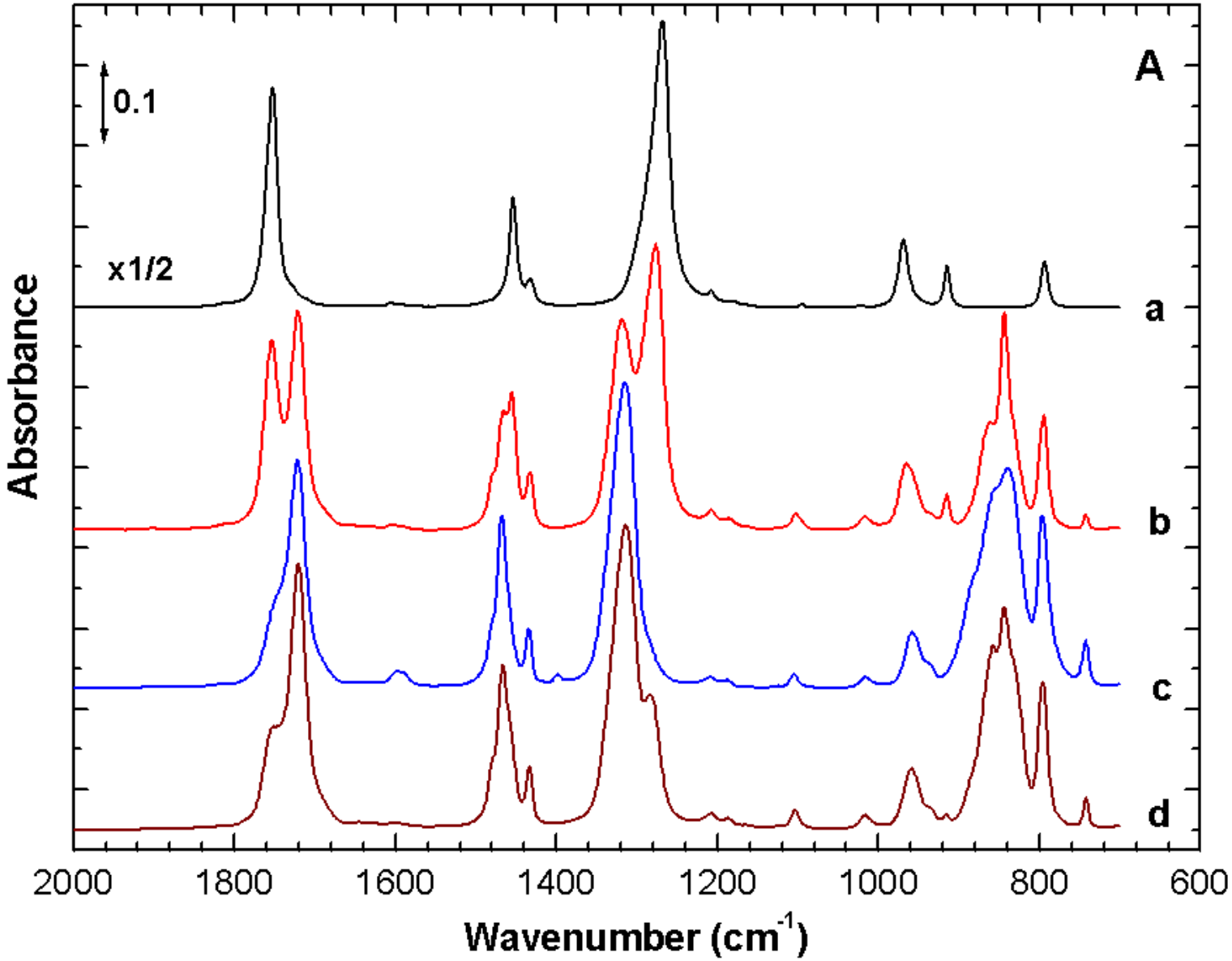

Duesenfeld Ex. 2008-027

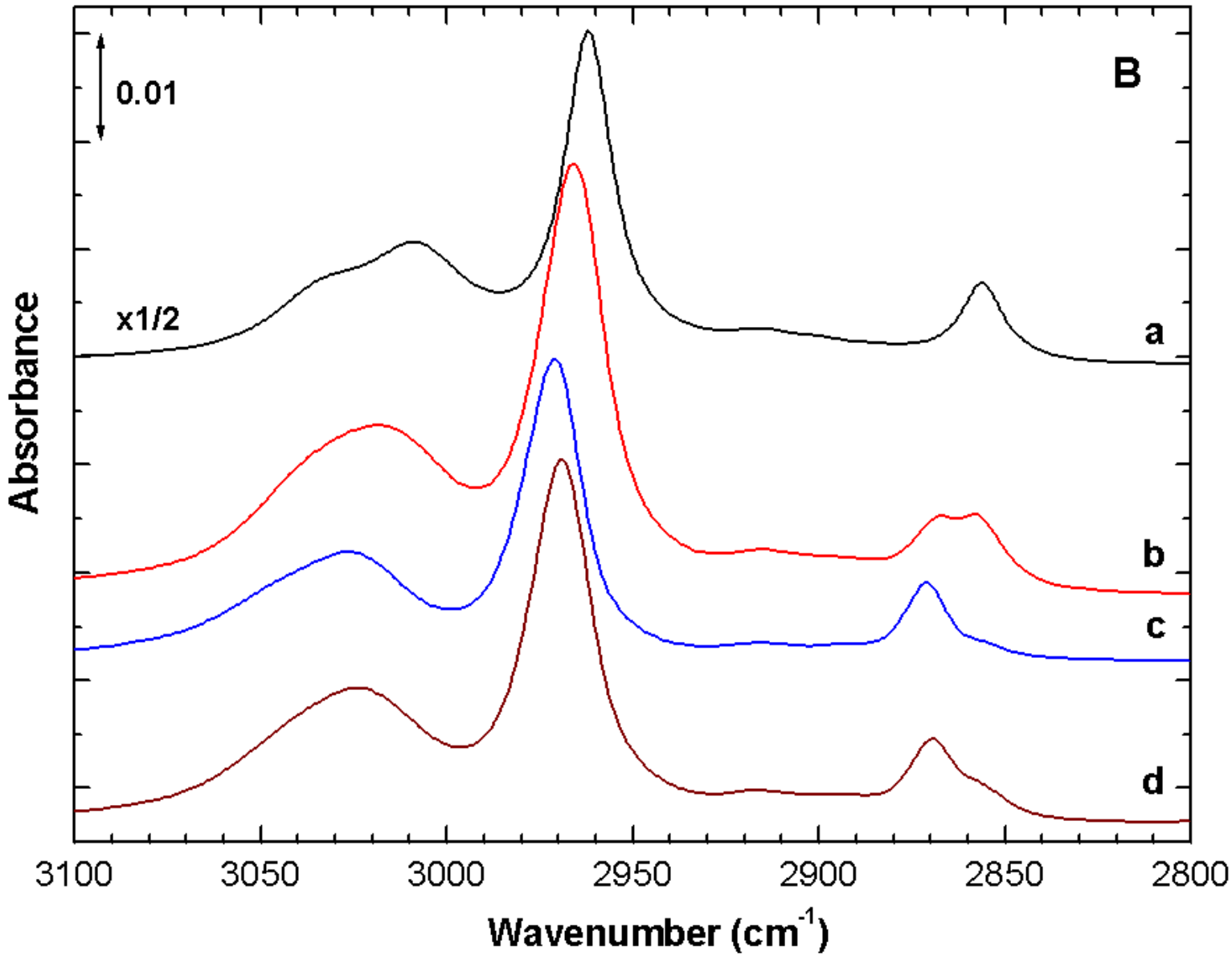

Duesenfeld Ex. 2008-028

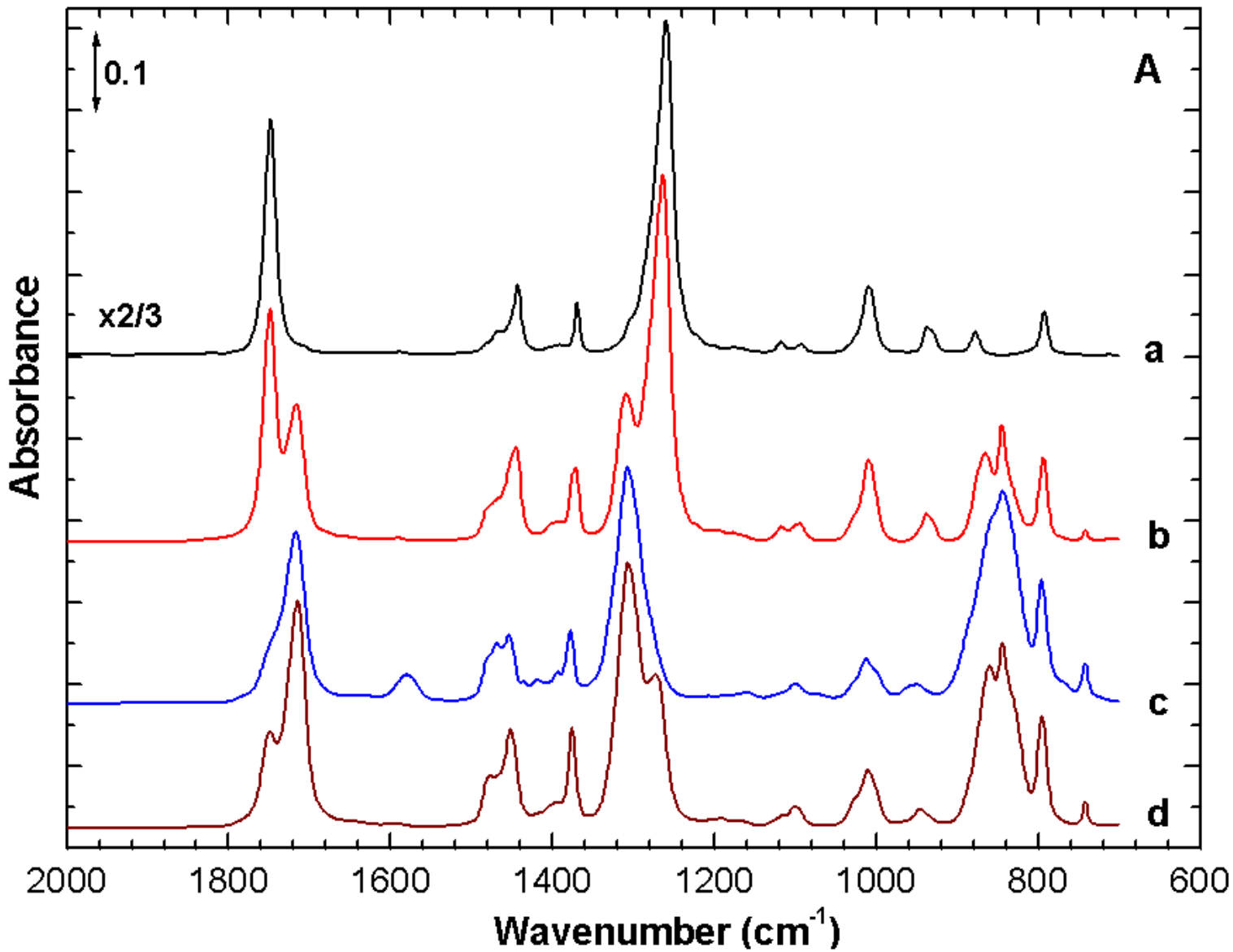

Duesenfeld Ex. 2008-029

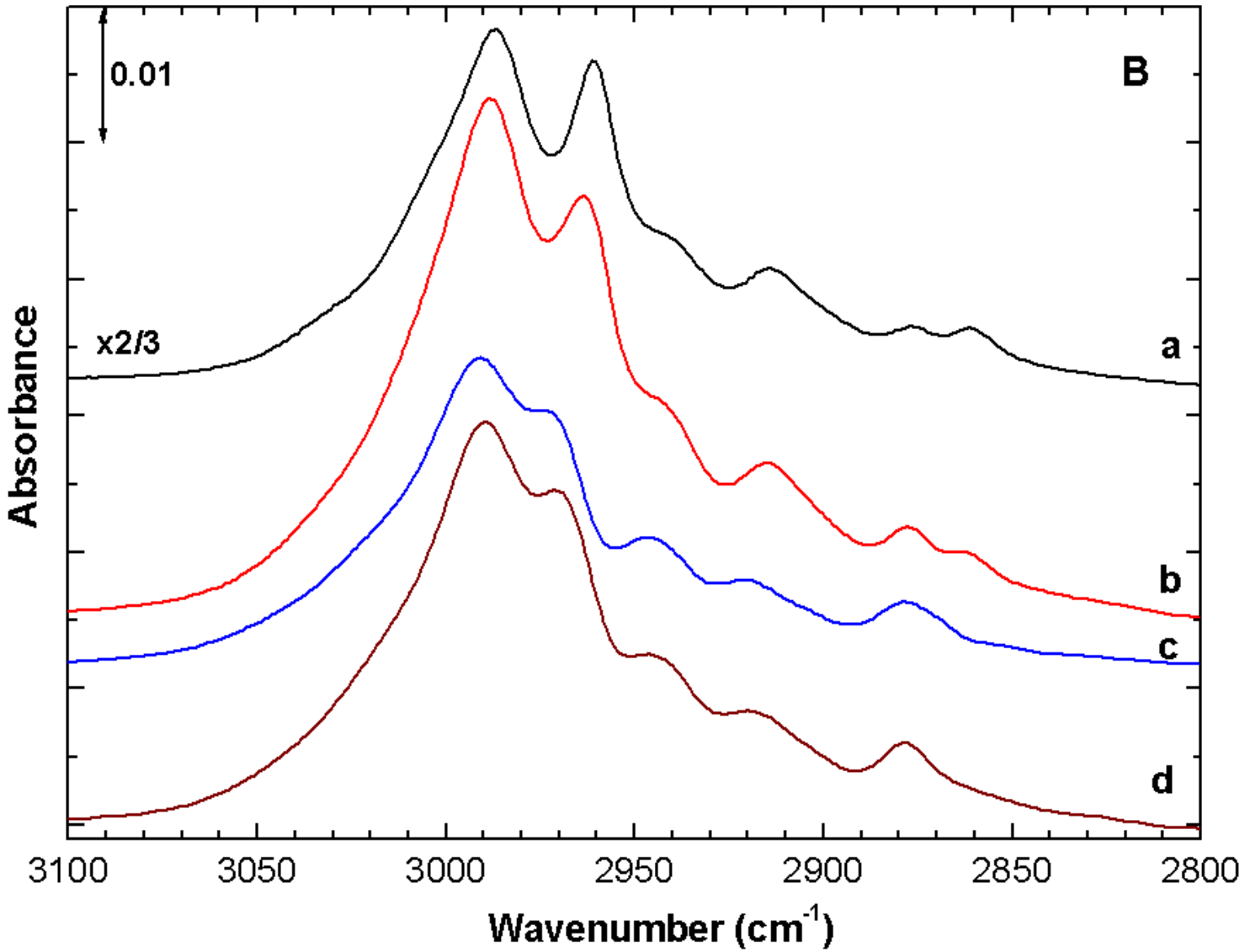

Duesenfeld Ex. 2008-030